Biotechnology Journal
www.biotechnology-journal.com

Biotechnol. J. 2017, 12, 1600471

DOI 10.1002/biot.201600471

Research Article

High throughput inclusion body sizing: Nano particle tracking analysis

Wieland N. Reichelt[1], Andreas Kaineder[1], Markus Brillmann[1], Lukas Neutsch[2], Alexander Taschauer[4], Hans Lohninger[3] and Christoph Herwig[1,2]

[1] Christian Doppler Laboratory for Mechanistic and Physiological Methods for Improved Bioprocesses, Institute of Chemical Engineering, Vienna University of Technology, Vienna, Austria
[2] Research Division Biochemical Engineering, Institute of Chemical Engineering, Vienna University of Technology, Vienna, Austria
[3] Research Group Electronic Media; Institute of Chemical Technologies and Analytics; Vienna University of Technology, Vienna, Austria
[4] Division of Clinical Pharmacy and Diagnostics, University of Vienna, Vienna, Austria

The expression of pharmaceutical relevant proteins in *Escherichia coli* frequently triggers inclusion body (IB) formation caused by protein aggregation. In the scientific literature, substantial effort has been devoted to the quantification of IB size. However, particle-based methods used up to this point to analyze the physical properties of representative numbers of IBs lack sensitivity and/or orthogonal verification. Using high pressure freezing and automated freeze substitution for transmission electron microscopy (TEM) the cytosolic inclusion body structure was preserved within the cells. TEM imaging in combination with manual grey scale image segmentation allowed the quantification of relative areas covered by the inclusion body within the cytosol. As a high throughput method nano particle tracking analysis (NTA) enables one to derive the diameter of inclusion bodies in cell homogenate based on a measurement of the Brownian motion. The NTA analysis of fixated (glutaraldehyde) and non-fixated IBs suggests that high pressure homogenization annihilates the native physiological shape of IBs. Nevertheless, the ratio of particle counts of non-fixated and fixated samples could potentially serve as factor for particle stickiness. In this contribution, we establish image segmentation of TEM pictures as an orthogonal method to size biologic particles in the cytosol of cells. More importantly, NTA has been established as a particle-based, fast and high throughput method (1000–3000 particles), thus constituting a much more accurate and representative analysis than currently available methods.

Received	06 AUG 2016
Revised	06 MAR 2017
Accepted	16 MAR 2017
Accepted article online	16 MAR 2017

Supporting information available online

Keywords: Electron microscopy · Grey scale image segmentation · Inclusion body · Nano particle tracking analysis · Stickiness

1 Background

The production of biosimilars is one of the main growth markets in pharmaceutical industry. Especially *Escherichia coli*, as well characterized expression host, has been established as easily accessible host for fast and efficient, high titer protein production. Hereby, high titer expression of heterologous protein frequently leads to inclusion body (IB) formation. This protein aggregation either coincides with high cytosolic concentrations of unfolded protein or can be induced, using a protein tag in order to reduce the toxicity of an otherwise toxic protein. However, while USP is hardly affected by IB formation, DSP

Correspondence: Prof. Christoph Herwig, Research Division Biochemical Engineering, Institute of Chemical Engineering, Vienna University of Technology, Gumpendorfer Strasse 1A/166-4, 1060 Vienna, Austria
E-mail: christoph.herwig@tuwien.ac.at

Abbreviations: BSA, bovine serum albumin; **DLS**, dynamic light scattering; **DSP**, down stream processing; **EDTA**, ethylenediaminetetraacetic acid; **FL**, fluorescence; **HPF**, high-pressure freezing; **IB**, inclusion body; **IPTG**, isopropyl-β-D-thiogalactopyranosid; **NTA**, nano particle tracking analysis; **PBS**, phosphate buffered saline; **TEM**, transmission electron microscopy; **USP**, up stream processing

constitutes the bottleneck in IB related production processes [1] and causes the bigger share of the total production costs.

As end product of USP, IBs are isolated by cell disruption prior to further processing during DSP. Industrial IB isolation is commonly conducted using high-pressure homogenization [2] and a continuous centrifugation to release and isolate IBs from the cells. Hereby, the continuous addition of washing buffer allows the combination of cell disruption and the removal of cellular debris in one unit operation. Post isolation, IBs are commonly solubilized in a chaotropic solubilization buffer, prior to refolding the protein into the native and therefore active protein conformation.

Integrated bioprocess development [7] strives to debottleneck the production process and to increase efficiency by addressing the impact of USP on DSP [8, 9]. This calls for sensitive response parameters describing the characteristics of IBs as intermediate product of USP and DSP. Solubilization in particular, as well as, refolding efficiency and purity appear to impair yields during DSP, which is why these steps and their efficiency have been investigated comprehensively [3–6].

Various methods have been investigated in order to characterize IBs, by paying attention to their different chemical properties. IB purity directly affects the necessary effort for further purification post-refolding and can be easily analyzed by SDS-PAGE [10]. Furthermore, IB solubility is critical for DSP performance, since highly soluble IBs would dissolve during the washing steps. In contrast, barely soluble IBs require high amounts of chaotrope reagents during solubilization, which increases buffer volume for refolding [11]. The increased volume in turn calls for bigger column diameters of economically expensive DSP purification columns [12]. Recent developments have enabled the concise measurement of solubility in respect to time [6, 8] as well as in respect to the concentration of chaotrope reagents [13].

Presumably mainly physical IB particle properties such as particle size and stickiness impact the yield of the isolation step prior IB solubilization during DSP. Nevertheless, the majority of available methods measure properties of the IB mass rather than properties of single particles. To date, analytical methods to quantify physical properties like the size and shape of IBs appear as being less developed.

Although a lot of effort has been invested especially into the quantification of IB size [14–18], the current, established methods have hardly been challenged/verified by an orthogonal verification method or are not single particle based (OD, DLS). Within this contribution we aim to establish an orthogonal verification method to analyze the size of large numbers of IBs and to assess sensitivity and information content of the nano particle tracking analysis (NTA) as a high throughput method to analyze IBs.

Besides being sensitive, a suitable method to effectively characterize the physical properties of IBs needs to be robust and reproducible. Mainstream adoption in academic as well as in industrial labs will only happen if the method is sufficiently simplistic. Highly sophisticated methods often lack technical transferability and comparability due to a certain degree of equipment and operator dependency.

1.1 Centrifugation based techniques

Early studies used centrifugation techniques, as centrifugal disc photo sedimentation [19] or cumulative sedimentation analysis [17], but require a particle density for the calculation of a size distribution of IBs. The more recently discussed approach of using an analytical centrifuge for IB sizing also relies on the density [20]. This dependency on IB density calls for an additional analytical method for IB density measurement, which makes methods relying on the density more laborious and less direct.

1.2 Dynamic light scattering

Dynamic light scattering (DLS) has extensively been utilized to size biological nano particles [11, 13–15, 21, 22]. Nevertheless, since this method only measures one variable its sensitivity is greatly impaired by multimodal distributions as well as by background particles [17]. As a counteraction, sample purification by serial washing steps [11, 13] or full-grown purification techniques as ultracentrifugation [15] have been investigated but these measures increase the risk of a measurement bias caused by sample preparation.

1.3 Field flow fractionation

Field flow fractionation (FFF) as separation or purification technique, as described elsewhere [23], has a wide dynamic range from 0.3–100 µm of particle separation capacity. The separation mechanism is a combination of Brownian motion, sedimentation and hydrodynamic lift forces [23] and facilitates bulk separation of nano particles according to their respective size and mass. Luo et al. used asymmetrical FFF in combination with multi-angle light scattering in order to analyze the size distribution of GFP inclusion bodies in response to induction time and temperature [14]. Using a sedimentation FFF in combination with a UV-Vis detector Margreiter et al. investigated the impact of inducer concentration and induction time on IB size [16]. Thereafter, an increase in the median spherical diameter of up to 140 nm over induction time was observed. Nevertheless, the effort for FFF method establishment is substantial and the potential interplay of different separation mechanisms implies that the interpretation of the results may not be so straightforward.

1.4 Imaging/TEM

The majority of the previously described methods and research contributions feature transmission electron microscopy, in an attempt to verify drawn conclusions. TEM facilitates conclusions based on single particle analysis by making single IBs visible. Given the overall goal of IB analytics of characterizing IBs as product of USP, the IBs should be analyzed in the most native conformation possible. Hereby, imaging of IBs in the cytosol excludes most of the otherwise necessary sample preparation and therefore a potential analytical bias. Nevertheless, it is indicated to analyze as many IBs per sample as possible in order to obtain a statistical representation of the IB population in the sample. Sizing IBs using TEM is commonly based on a laborious manual image analysis of the TEM image [16, 24]. In addition, the effort for sample preparation, the analytical technique, and image evaluation is substantial and basically excludes the possibility of using the usage of EM-based methods as routine analytical technique.

1.5 Nano particle tracking analysis

In this contribution we introduce nano particle tracking analysis (NTA) [25] as method to analyze and size a large number of biologic nano particles individually. For biologic particles the dynamic range of NTA spans 100–1500 nm, which fits the reported size range of IBs from 170 to 1300 nm [13, 16, 19, 24]. NTA uses a laser as light source, which passes through the sample particle suspension and illuminates the particles. In scatter mode, the scattered light, while in fluorescence mode the emitted light is recorded by a high-speed camera through a microscope. Due to the angle between the light beam and the camera axis, individual particles can be tracked and analyzed. At a constant temperature and a constant viscosity of the liquid, the size of each particle correlates to the Brownian particle movement. Using the Stokes–Einstein equation, the individual particle size can consequently be calculated resulting in a histogram of the particle size distribution of the particles in suspension.

The overall goal of this contribution is to provide a cost and time efficient method to quantify IB size. Firstly, for method verification, we aim to establish grey scale image segmentation of TEM pictures as an orthogonal method to assess IB size. Secondly, as cost and time efficient method, NTA is assessed as method to quantify IBs and their size in the background of cell debris. Finally, as an exemplary application the growth of IBs is investigated over process time.

2 Materials and methods

2.1 Bioreactor system

The fermentations were conducted in a DASGIP multi-bioreactor system (4Force; Eppendorf; Germany) with a working volume of 2 L each. The DASGIP control software v4.5 revision 230 was used for data logging and control: pH (Hamilton, Reno, USA), pO2 (Mettler Toledo; Switzerland;), temperature and stirrer speed (module DASGIP TC4SC4; Eppendorf; Germany), aeration (module DASGIP MX4/4; Eppendorf; Germany) and pH (module DASGIP MP8; Eppendorf; Germany). CO_2, O_2 concentrations in the off-gas were quantified by a gas analyzer (module DASGIP GA4; Eppendorf; Germany) using the non-dispersive infrared and zircon dioxide detection principle, respectively.

2.2 Cultivations

A recombinant BL21 DE3 *E. coli* strain was cultured, producing an intracellular protein (≈30 kDa) in the form of inclusion bodies, after a one-time induction with IPTG (1 mM). The synthetic media was based on the recipe from Korz et al. [26], where the limiting C-source was glucose.

Pre-cultures were grown to a OD600 of approx. 1.5 in 150 mL media. 2.5% of the batch volume was added as pre-culture for inoculation. The strain was cultivated at a controlled pH level, dissolved oxygen DO_2 (>30%) and temperature. The DO_2 was kept over 30% by supplementing oxygen to the air. After depletion of the C-source in an initial batch phase, the pre-induction fed-batch was started. The pre-induction feeding strategy was based on an exponential feed forward profile to maintain a predefined growth rate [27]. Upon induction, stirrer speed was set to 1400 rpm and aeration to 1.4 v/v/m for the whole process. The pH was maintained by adding 12.5% NH_4OH, which also served as nitrogen source.

2.3 Imaging

For high-pressure freezing (HPF) *E. coli* samples were pelleted and re-suspended in 5% BSA. After a second centrifugation step, the pellet was immediately frozen in a high-pressure freezer (HPF Compact 01; Wohlwend; Switzerland). The samples were then transferred into a freeze substitution unit (EM AFS2; Leica Microsystems; Germany) for water substitution with 2% uranyl acetate in anhydrous acetone over five days (–140°C to –90°C for 3 h; –90°C to –90°C for 25 h; –90°C to –54°C for 18 h; –54°C to –54°C for 8 h; –54°C to –24°C for 10 h; –24°C to –24°C for 15 h; –24°C to 0°C for 12 h;0 to 0 for 2 h)

For chemical fixation, the supernatant of the pelleted *E. coli* samples was carefully aspirated and cells were fixed using 2.5% glutaraldehyde in 100 mM cacodylate

buffer at pH 7.4 for 1 h at room temperature. After washing in the same buffer samples were post-fixed in 2% osmium tetroxide in cacodylate buffer, washed and dehydrated in a graded series of ethanol.

The dehydrated specimens were embedded in agar 100 resin (AGR 10131; Agar Scientific Ltd; UK) and after hardening, ultrathin sections (70 nm) were prepared (Leica ultramicrotome UCT; Leica Microsystems; Germany). The 70 nm sections were collected on 100 mesh Cu/Pd grids with a supporting formvar film. Sections were post-stained with 2% aqueous uranyl acetate, followed by incubation with Reynold's lead citrate. Images were collected using a transmission electron microscope (Morgagni 268D; FEI; Netherlands) operated at 80 kV and equipped with an 11 megapixel camera (Morada CCD; Olympus-SIS; Germany). Images were collected in both, regions of random sections and regions of one section.

2.4 Image segmentation

To quantify the IB size, the relative area of IB per cell was calculated based on grey scale image segmentation. The thresholds for background and IBs were selected manually by the operator, specific for each picture. The difference in area of the background and total image area corresponds to the area covered by cells. A pre-test with a larger number of operators (9) substantiated that the image segmentation is insignificantly impacted by the operator and can be regarded as transferable in-between operators (data not shown). Image segmentation of the 17 different samples and one negative sample with three to six images for each sample was conducted in Image Lab (v.1.02, Epina GmbH, Pressbaum, Austria; http://www.imagelab.at). 160–380 individual cells were repetitively analyzed per sample.

2.5 Cell disruption

2 mL of the fresh culture broth were centrifuged (4500 × *g*; 10 min; 4°C). The cell pellets were re-suspended in 20 mL 0.1 M Tris-buffer; 10 mM EDTA (pH 7.4) buffer and were disrupted in a high-pressure homogenizer (EmulsiFlex; Avestin; Canada) at 1400 ± 100 bar in six passages. For chemical fixation, 0.2% glutaraldehyde (G7776; Sigma Aldrich; Austria) was added dropwise to the re-suspended pellet and incubated 1 h at 4°C prior to homogenization.

2.6 Fluorescence stain

To discriminate cell debris from IBs, the homogenized cell pellet (5000 × *g*; 5 min) was re-suspended and incubated for 30 min in a 1x PBS solution containing 1% BSA and 2.2 mg/L of a product specific biotinylated primary antibody (courtesy of Sandoz GmbH; Austria). After washing with 1x PBS 1% BSA once, the pellet was re-suspended and incubated for 30 min in 1x PBS 1% BSA containing 10 µg/mL secondary IgG antibody labelled with Alexa 488 (AT11001; Invitrogen Life Technologies; Austria). Prior to measurement, the suspension was washed and re-suspended in 1x PBS.

2.7 Nano particle tracking (NTA)

A NS500 (Malvern, UK) software release (Nano Sight 3.0) equipped with a 488 nm laser and a CMOS camera (Hamamatsu Photonics, Japan) was used for the conducted NTA measurements. Most of the software parameters and algorithms are proprietary and are not known to the authors. The measurement chamber was primed prior to each measurement with 1x PBS to minimize particle drift. In-between measurements the chamber was flushed twice to avoid sample carryover. All samples were sonicated 1 min prior to measurement and diluted 1:10 in PBS. The focus level was set automatically, a standardized camera level of 16 was used in combination with a detection threshold of 20. Six replicates, 90 s each were measured with a 5 s time delay at a controlled temperature of 25°C.

2.8 Titer quantification

Product titer was measured using RP-HPLC after solubilizing the washed pellet of disrupted cells in guanidine hydrochloride. To calculate the specific titer, biomass concentrations were gravimetrically quantified after drying at 105°C for 72 h. Therefore 2 mL of culture broth were centrifuged (4500 × *g*, 10 min, 4°C) in a pre-weighted glass tube and the pellet was washed once with 5 mL RO water. The determination was done in duplicates. After drying in the drying oven, the biomass dry weight was measured on a scale.

2.9 Statistical data analysis

Data were subjected to statistical analysis using Datalab Version 3.5 (Epina GmbH, Pressbaum, Austria, http://datalab.epina.at/). Based on an $\alpha = 0.05$ the significance of the correlation was evaluated based on the p-value. Data were not transformed. Serial correlation was tested using the Durbin-Watson statistic.

3 Results

3.1 TEM+HPF as a gentle method for IB visualization

Currently, there is no verified method available to quantitatively size a representative number of IBs. This circumstance hinders the establishment of a high throughput method for quantitative IB sizing. Consequently, method

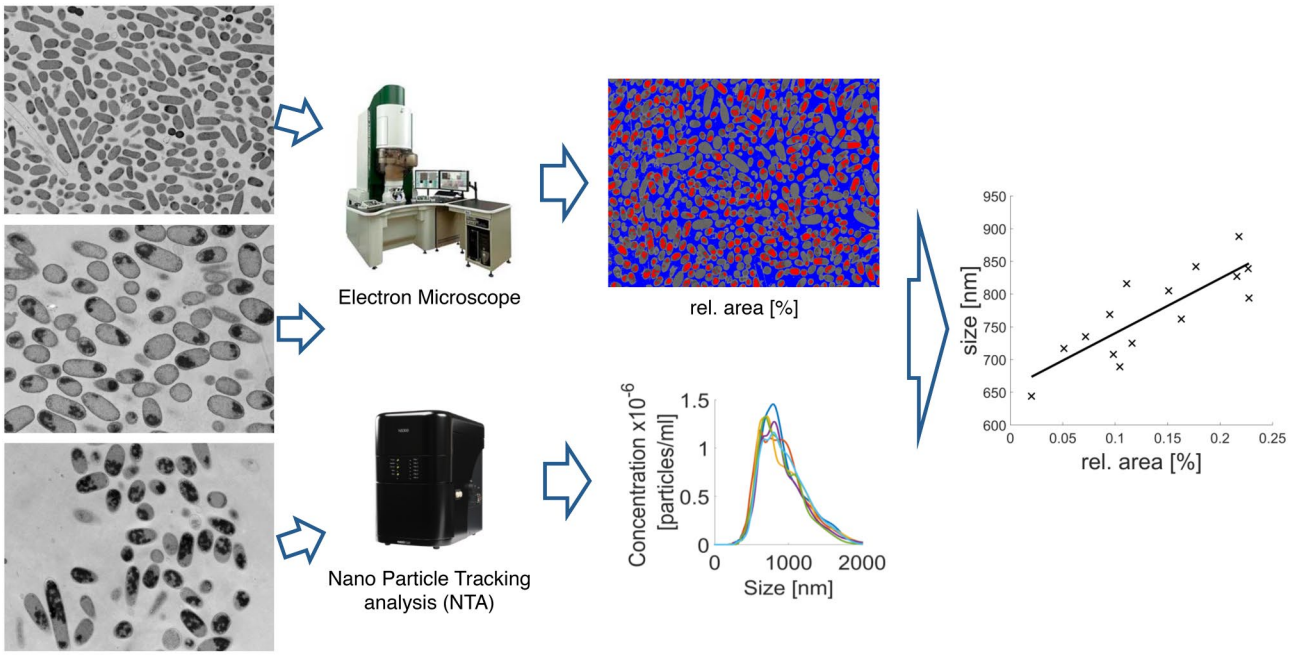

Figure 1. Method assessment by relative method verification. Flow chart of the targeted relative verification of NTA and TEM derived quantification of IB size. Independent IB process samples are analyzed by NTA as well as by TEM. TEM images on the left only represent the IBs as such, not the method specific sample preparation. While NTA measures IBs in the background of homogenized cells (Supporting information 2), the verification method TEM is based on ultrathin sections of whole cells in combination with grey scale image segmentation (Supporting information 1). NTA yields the hydrodynamic particle diameter distribution which corresponds to the IB size (nm) based on the utilized specific FL stain. TEM derived images of process samples are segmented according to the grey scale. Based on the image segmentation of IB area and cell area the relative area IB/cell [%] is calculated.

assessment can only be based on relative confirmation by comparing the results of two otherwise orthogonal methods (Fig. 1). Since an absolute measurement method for the particle size of a distribution of biologic nanoparticles is not available, a relative verification is targeted by comparing the relative area (%) derived from TEM and the hydrodynamic diameter (nm) derived from NTA. To avoid measuring artefacts it is of utmost importance to minimize the impact of sample preparation in order to preserve the most native IB form. While TEM is capable of visualizing IBs even in the cytosol, NTA can only measure particles in suspension. For this reason, HPF has been used as fixation approach for TEM, due to the gentle fixation properties. Supporting information 1 illustrates the conservation of cellular structures for different induction time points of two representative experiments. In contrast, sample preparation for NTA requires cell homogenization and a consequent FL stain in order to facilitate IB analysis in the background of cell debris.

3.2 Grey scale image segmentation for quantitative IB sizing is not significantly operator dependent

Based on deduced the images from Supporting information 1, qualitative IB growth over time can be observed. But for a quantitative assessment of IB size/growth over time, a standardized approach for IB sizing is necessary. Using grey scale image segmentation from TEM images. The relative IB size was quantified as IB area per cell (%). Basal grey values of TEM images, have been found to be highly variable owned to background particles. This impairs a uniform background correction and consequently fully automated image segmentation. Targeting a sound science method to reproducibly quantify cytosolic IB size, the operators analyzed 17 independent samples by image segmentation (Fig. 2) . Using a software aided approach, the time per image segmentation decreased below 10 s. For each sample three to six TEM images were recorded and segmented by the individual operator in random order at least three times. In Fig. 2A–C the variance induced by the different operators is indicated. The respective results are not statistically significant operator dependent, rendering the method transferable between operators for IB sizing and thereby suitable for method verification. Consequently, TEM imaging using HPF as gentle fixation method for IBs in combination with the software aided image segmentation approach across operators, was employed as orthogonal verification method.

In order to minimize artefacts, sample preparation was simplified as far as possible. While mere homogenization and direct NTA measurement did not lead to satisfying results, the implementation of a FL stain increased sensitivity of the method (data not shown). Also, standard FL beads were identified with high precision even in the

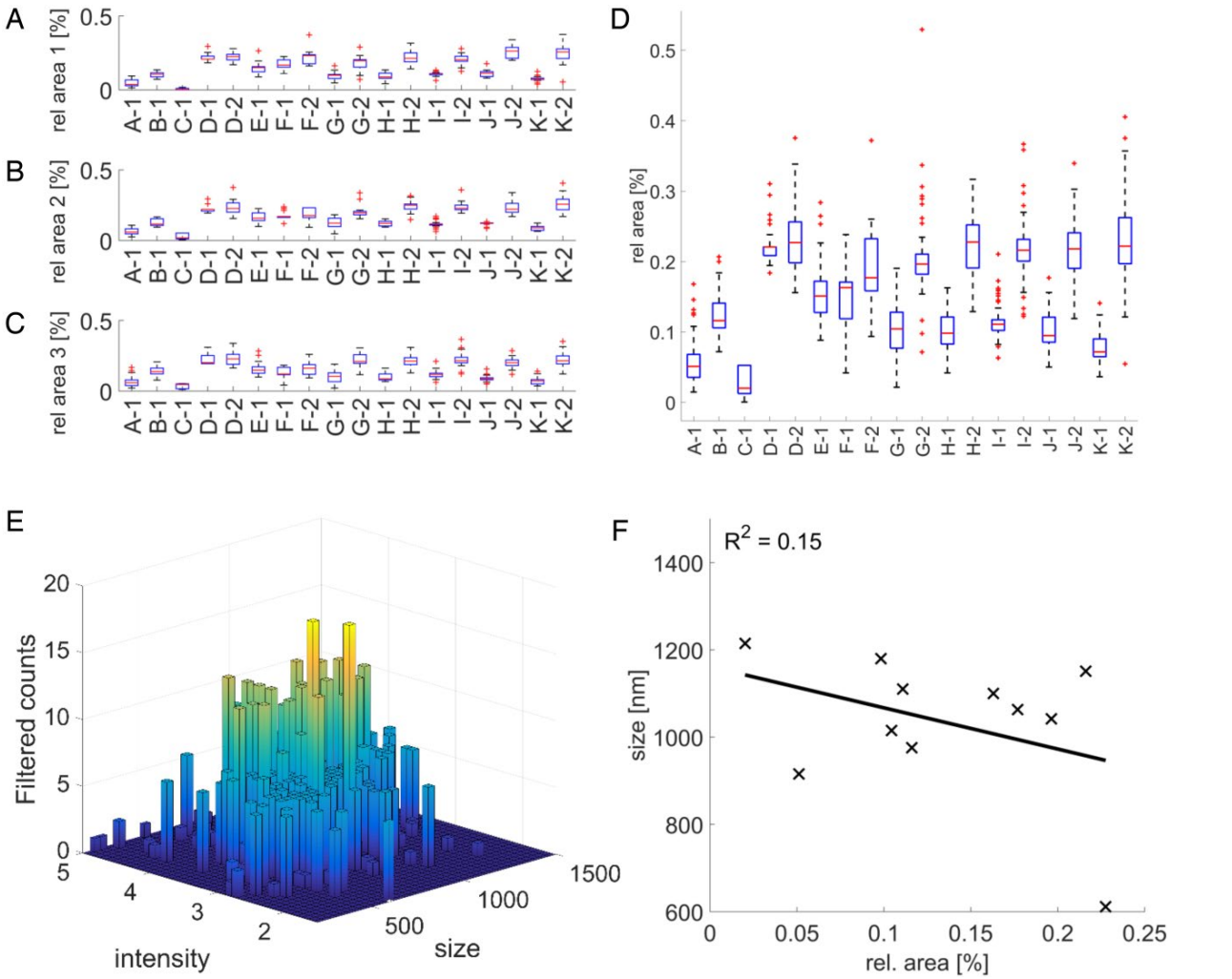

Figure 2. Grey scale image segmentation of TEM images for IB sizing is not significantly operator dependent. The relative area (rel. area [%]) corresponds to the area covered by IBs per cell background, 17 induced samples and one negative sample (C-1), of each sample three to six individual TEM images were segmented in random order ($n > 3$), each letter corresponds to an individual fermentation, samples with the same letter but different number correspond to different time points; (**A**–**C**) Grey scale image segmentation results operator specific, each subpanel corresponds to one individual operator; (**D**) all segmentations (> 550) results pooled, whiskers indicate 75% interval; (**E**) Filtered data of the size distribution of fixated IBs by NTA in the background of cell debris, all tracked particles of one sample measurement including the six replicate measurements, filtered by intensity and track length. (**F**) The correlation of relative IB area (%) to the hydrodynamic diameter derived from NTA (nm) was not found to be significant $p(t) = 0.18$, also the residuals were not found to be normally distributed.

background of stained homogenate (data not shown). Consequently, the samples were measured post homogenization and FL stain without any fixative (non-fixated). To illustrate the data basis for a size measurement by NTA, Fig. 2A displays a histogram of tracked and sized particles of an exemplary FL stained sample. Although a high number of particles was tracked in high number, NTA results and the relative IB areas from TEM-HPF were not significantly correlated (Fig. 2F). Judging from the TEM-HPF images (Supporting information 1) as well as from the image segmentation (Fig. 2D), a significant difference/growth over time in size of IBs can be observed. Nevertheless, this trend was not represented by NTA results.

3.3 Particle fixation for nano particle tracking analysis (NTA) increases method sensitivity

To investigate the impact of sample preparation on IB sizing by NTA, additional tests were conducted using a chemical fixative prior to cell homogenization. The IB sizing results of non-fixated IBs and chemical fixated IBs are compared in Fig. 3. Figure 3A and 3B illustrate the massive improvement of NTA raw data quality upon sample fixation prior to homogenization. The standard deviation is decreased and displays significantly less variance (Fig. 3C). Highly interesting is the observation that fixated samples display quantitatively more unspecific particles

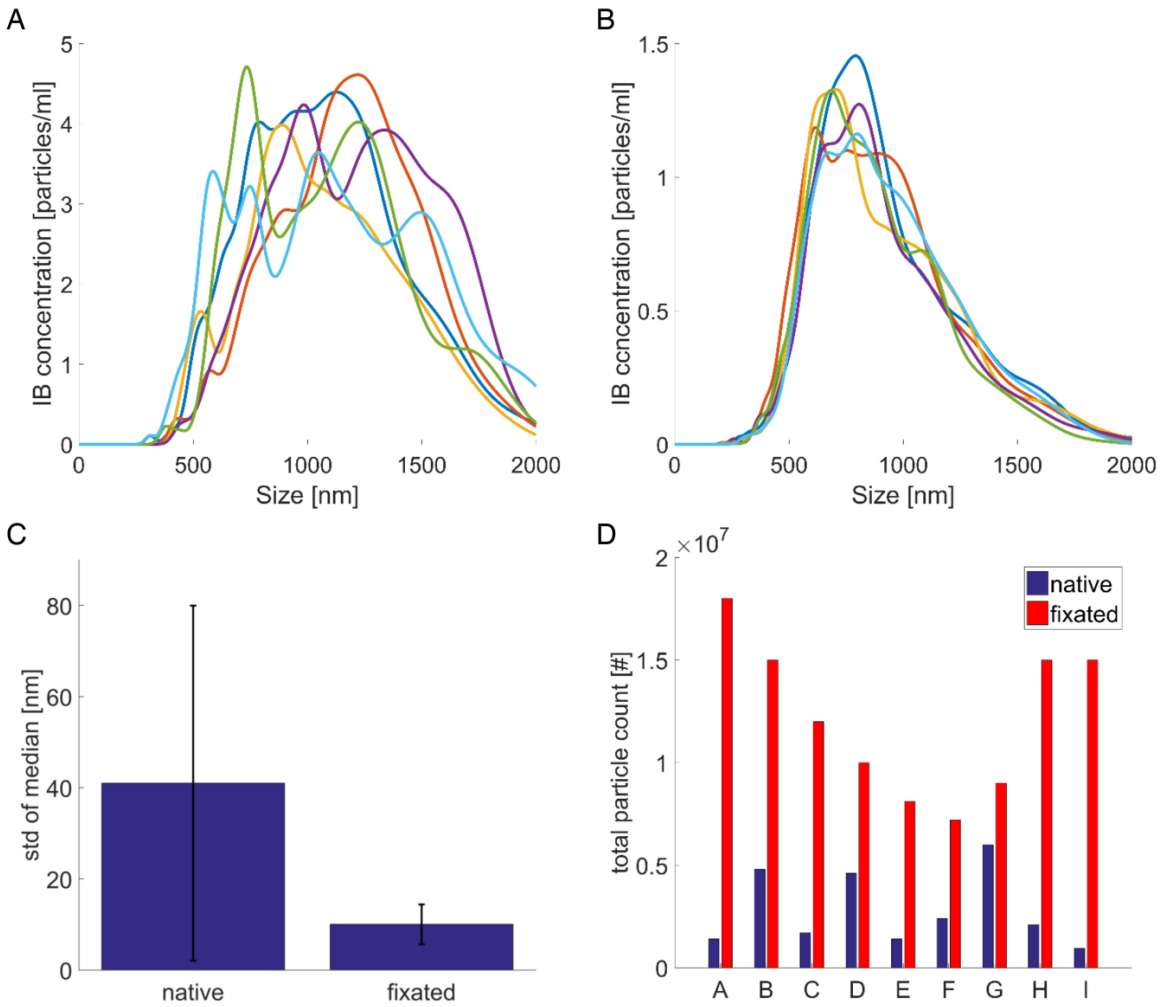

Figure 3. The positive impact of fixation prior to homogenization on NTA particle measurement. (**A**) raw data of particle size distribution of FL stained non-fixated IBs; (**B**) raw data of particle size distribution of FL stained fixated IB of the same sample as in (**A**); (**C**) Fixation prior to homogenization decreases standard deviation of the median size and boosts reproducibility, comparison of the standard deviation of the median of the particle size distribution of the six replicate measurements per sample, for not fixated (native) $n = 37$ and fixated (fixated) $n = 26$ samples, $p(t) < 0.001$; (**D**) total unspecific particle counts of NTA raw data, A-I correspond to sample names from various fermentations and time points, the observed trajectory in the particle count of fixated samples is presumably of coincidental nature.

than non-fixated samples (Fig. 3D). This is surprising in respect of the cross-linking properties of glutaraldehyde, which in theory should lead to generally bigger and fewer particles. Possibly, the addition of a fixative prior to homogenization prevents IBs from aggregating post homogenization during sample preparation.

Besides increasing measurement sensitivity, sample fixation appears to impact the intensity per particle (Fig. 4A). In order to put the IB size obtained from fixated samples into perspective, Fig. 4B illustrates the correlation of all measured TEM and NTA samples. Based on a p value of 0.002, it can be concluded that the rel. IB area (%) and the hydrodynamic diameter (nm) are correlated. To illustrate that the measured IB size is not a redundant measure of a simple titer quantification, the TEM areas as well as the IB diameters derived from NTA are compared to the respective specific titers (Fig. 4B and 4C). Based on the assumption of a uniform IB density within one sample the size of IBs should be tightly correlated to the amount of product contained in the particle. Nevertheless, the specific product titer does not display a highly significant correlation to the particle size, neither for particle sizes derived from TEM (Fig. 4C) nor from NTA (Fig. 4D).

The analysis of early and late time points of induction from different sets of experiments increases the observable differences in IB size. In comparison, the timely resolution of size over induction time is a greater challenge in regard to method sensitivity. In this respect, Fig. 5A illustrates the growth of IB size as well as the progression of specific product titer (g/g) over induction time. In accordance with Fig. 4D the IB size and product titer were not found to be

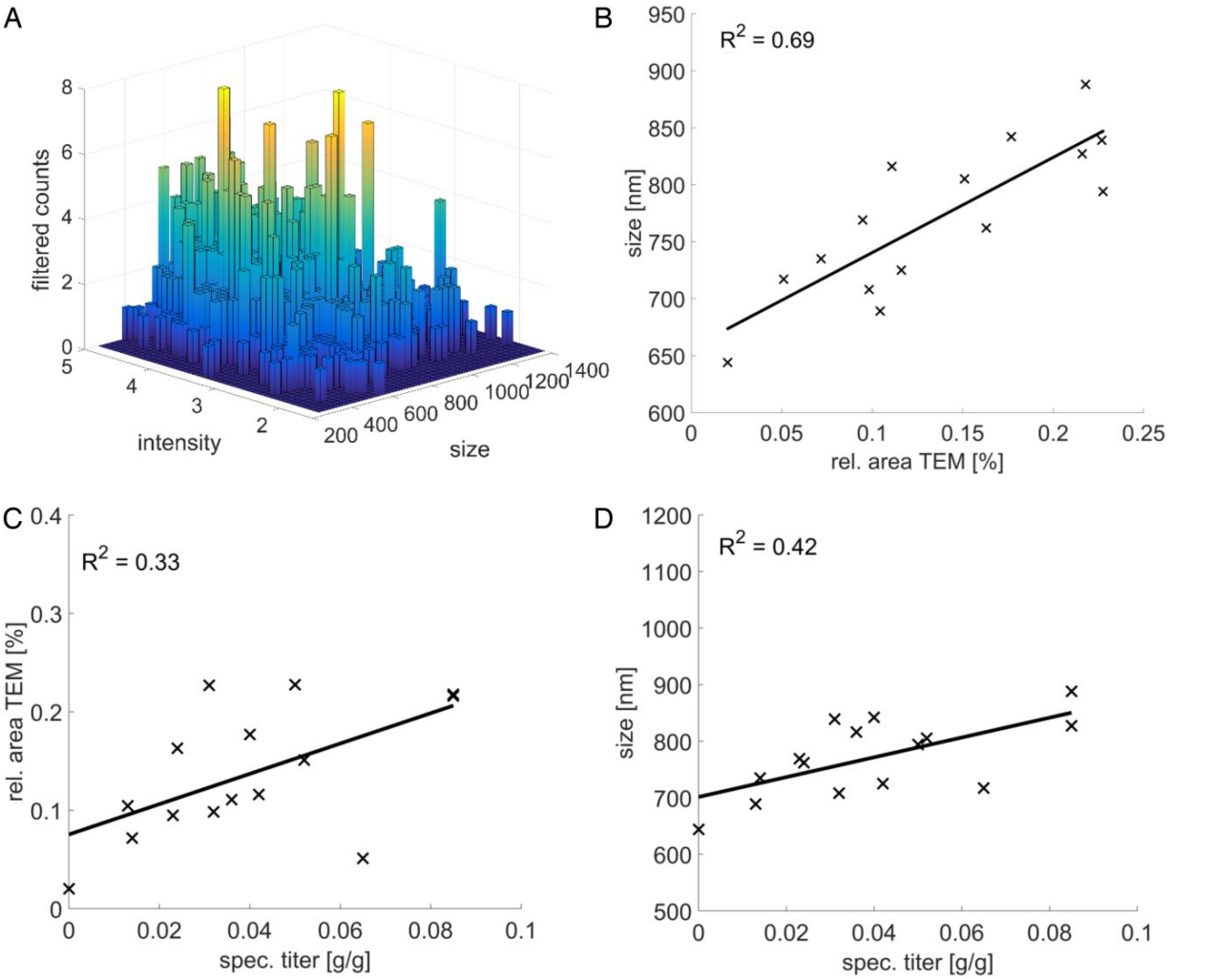

Figure 4. IB size of fixated samples derived from NTA is significantly correlated to the relative IB area derived from TEM; (**A**) Filtered data of the size distribution of fixated IBs by NTA in the background of cell debris, all particles of one sample measurement including the six replicate measurements, filtered by intensity and track length; (**B**) significant correlation of relative area (rel. area TEM [%]) and particle size derived from NTA (size), $n = 15$, $R^2 = 0.69$, $p(f) = 0.002$; (**C**) correlation of relative area (rel. area TEM [%]) and specific product titer (spec. titer [g/g]), $n = 15$, $R^2 = 0.33$, $p(f) = 0.026$, no serial correlation; (**D**) correlation of particle size derived from NTA (size) and specific product titer (spec. titer [g/g]), $n = 15$, $R^2 = 0.42$, $p(f) = 0.009$, no serial correlation.

closely correlated. The increase in size (+10 to 12%) was found to be comparably small given the substantial increase in specific titer (+300–400%) over induction time.

To investigate the impact of homogenization and correlated sample preparation on the sensitivity of the NTA measurement, additional samples after homogenization were analyzed (Fig. 5) by TEM. It can be observed that in case of HPF (Fig. 5C), the IBs are released into the supernatant and appear to maintain a more segregated state. The structure of these protein aggregates appeared poriferous and fragile. In contrast, the chemical fixation of the same sample prior to homogenization led to denser particles (Fig. 5B). Based on these images, it can be inferred that chemical fixation helps to maintain the IB conformation. A more pronounced impact of chemical fixation can be observed if the sample preparation for TEM is based on a thorough chemical fixation (Supporting information 3) instead of HPF/AFS (Supporting information 1). This conclusion is also in accordance with the previously discovered positive impact of fixation on NTA sensitivity.

4 Discussion

The investigation of the interface of USP and DSP requires sensitive analysis of the USP end product – the inclusion bodies. In this context, it are especially physical IB properties that presumably impact the isolation yield prior to solubilization and refolding during DSP. Accordingly, the goal of this contribution was to establish and verify a particle-based method to size a representative number of IBs with high sensitivity and high efficiency.

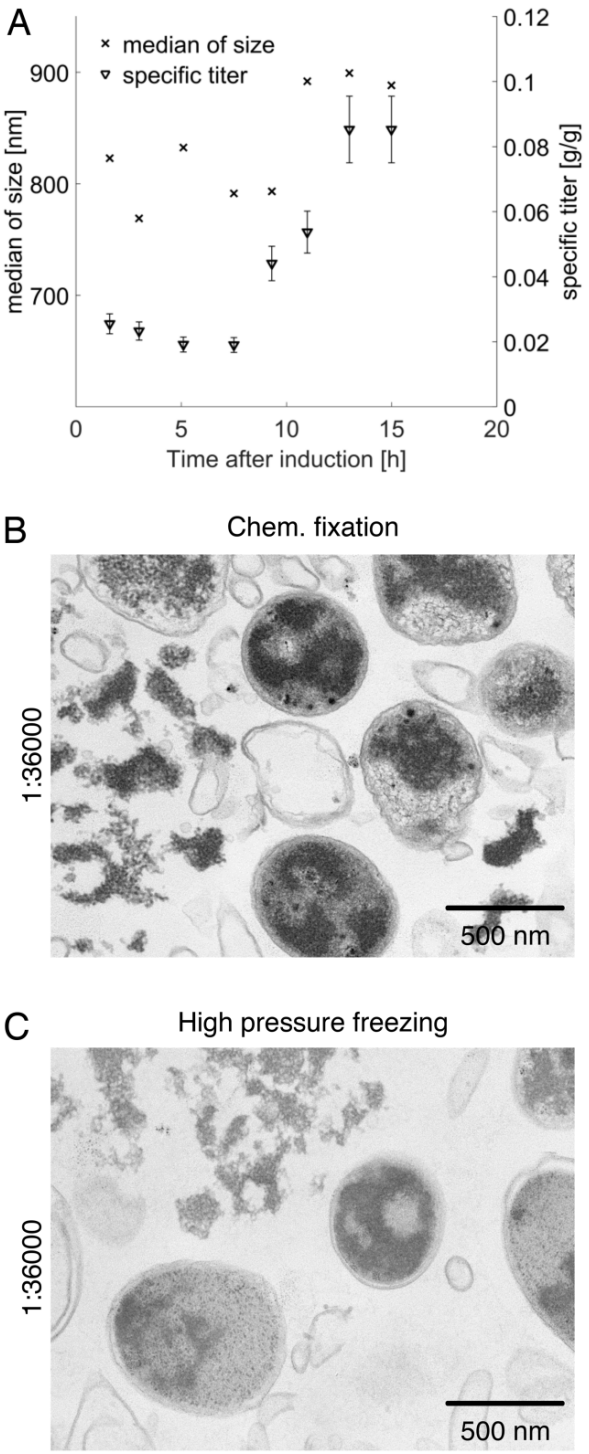

Figure 5. IB sizing by NTA features sufficient sensitivity to resolve IB growth over time; (**A**) The specific titer (spec. titer [g/g]) and IB size (median of size [nm]) over process time since induction (Time after induction [h]), as indicated before size and titer are correlated significantly, $n = 8$, $p(f) = 0.015$, including a serial correlation over time (**B**); Fixation leads to particle condensation in the homogenate as well as in the cells, TEM image of IBs after homogenization (700 bar, six passages) of chemically fixated cells, 1:36 000; (**C**) TEM image of IBs after homogenization (700 bar, six passages) of non-fixated cells, 1:36 000.

4.1 Grey scale segmentation of TEM images is a sensitive method for IB characterization

For method verification, a second, orthogonal method to assess IB size has been established. To minimize the effect of sample preparation and correlated artefacts, it was indicated to analyze the IBs in the most native conformation feasible. Using only centrifugation prior to HPF, sample preparation was reduced to a minimum. Besides sample preparation, the method of sample fixation has been a topic of vivid discussion. A common approach for sample fixation of IBs is chemical fixation [11, 13, 20, 24] or air drying of the specimen on a copper grid [15, 16]. Despite the wide usage of these methods, the specimen might be altered, subcellular structures can condense and shrinkage can occur. In this contribution, that used HPF-AFS, the structure of IBs was found to be far looser and more sensitive in contrast to the general opinion regarding the shape of IBs [13].

Regardless of the sample preparation, microscopy generally simplifies the shape of 3D specimens to 2D images. Although 3D-TEM offers an alternative, the effort per measurement renders 3D-TEM unfeasible for the analysis of over 100 particles per sample. To compensate for the drawback of a 2D image based method a representative number of particles needs to be analyzed. Especially since the IBs do not appear to have a fully symmetrical, spherical shape, different orientations need to be accounted for by sizing a larger number of IBs. Peternel et al [24] addressed the problem of the statistical significance and sized 250–350 IBs in order to obtain a histogram of IB size distribution of isolated and washed IBs. In accordance with this contribution, 160–380 individual cells (containing IBs) were analyzed repetitively by each of the three operators for every sample. But in contrast to the chemical fixation used by Peternel et al [24], HPF-AFS was used as a highly gentle method, renowned for its ability to preserve cellular substructures. Hereby, we established HPF-AFS TEM imaging of IBs in the cytosol in combination with grey scale image segmentation as valuable method to reproducibly quantify a representative number of IBs, independent of an operator. Nevertheless, the five days needed for sample preparation in combination with the undeniably time-consuming procedure of image segmentation, do not qualify the method as simplistic or easily transferable in a technological sense.

4.2 NTA is a sensitive method to size a representative number of IBs

IB sizing by NTA permitted the characterization of a representative number of particles (>1000) per sample. In contrast to HPF-AFS TEM, sample preparation for the NTA measurement as well as the actual measurement of several samples was done within one day. Data evaluation was fully automated and can be easily standardized,

which makes it less operator dependent. Consequently, NTA appears to offer a far more feasible approach to quantify IB properties on a single particle level, compared to currently available methods.

In the context of NTA measurements the chemical fixation of the cells prior to homogenization yielded an increase in sensitivity as well as a substantial increase in total, unspecific particle count. Although the total amount of recognized particles had increased (Fig. 3D), the amount of relevant particles (IBs) had decreased (Fig. 3A and 3B). This observation might be due to a certain aggregation tendency of native particles. This tendency could lead to an aggregation of the IBs with cell debris, especially in combination with a disintegration of the IBs triggered by shear stress during homogenization. Cellular debris after high-pressure homogenization is about 0.5 µm in size [17]. In combination with IB fragments, the resulting size would theoretically overlap with the expected size of native IBs. In case fixation impairs this aggregation and decreases the probability of IB disintegration during homogenization, fixation would lead to an increase in the total number of particles but a decreased number of product specific particles.

Despite using a product specific FL stain in combination with a chemical fixation of the cells, background particles were found to create a bias in the sizing of the standard beads present in the background of homogenate. The observed strong background signal might be attributed to a bleed through of scattered light through the long pass fluorescence filter, which decreases the method specificity. For future measurements, it would be advisable to circumvent such issues by increasing the distance between the excitation wavelength and fluorescence filter.

Besides the methodological advances for sizing IBs by using NTA and TEM, the results indicate that high-pressure homogenization greatly impacts IB properties. Consequently, the native size of the IBs is highly unlikely to be preserved throughout high pressure homogenization. Nevertheless, a tendency to adhere to surfaces (stickiness) during the isolation step, e.g. the wall of the continuous centrifuge, could cause significant product loss. This hypothesis substantiates the necessity of a sensitive characterization of IB particle properties, in order to enable the scientific community to investigate the correlated product loss.

The NTA method offers an approach to quantify the impact of USP and homogenization on the IB particle property size. Moreover, NTA allows to assess the ratio of particle count of non-fixated and fixated IB samples, which could potentially be used as a measure of stickiness.

In summary, the findings infer that even if different process parameters in USP elicit differences in IB particle properties, it is highly unlikely that these differences are preserved throughout high-pressure homogenization. However, IB sizing by NTA could help to better understand the molecular processes which lead to different aggregation tendencies and in turn, impact isolation efficiency. Consequently, NTA could be used to derive an additional response parameter on the basis of which integrated bioprocess development might succeed in investigating the interlink of USP and DSP.

4.3 Conclusions

The overall goal of this contribution was the establishment and assessment of a simplistic and sensitive method for high throughput IB sizing.

(i) TEM in combination with grey scale image segmentation is a sensitive and reproducible method to quantify the size of native, cytosolic IBs and can be used for method verification.
(ii) NTA is a particle-based method that allows to size a great number (>1000) of fluorescence labelled IBs in the background of cell debris.
(iii) Chemical fixation of IBs prior to homogenization leads to a decrease in standard deviation and particle count but increases the reproducibility of IB sizing with NTA.

Based on the observed effect of fixation, it can be hypothesized that high-pressure homogenization annihilates differences in IB size caused by USP. Nevertheless, the ratio in particle count of native homogenate and fixated homogenate offers a measure for IB stickiness.

We are grateful for the financial support of Sandoz GmbH. The TEM measurements were performed by the EM Facility of the Vienna Biocenter Core Facilities GmbH (VBCF), a member of Vienna Biocenter (VBC), Austria. We are grateful for the access to the NTA measuring device facilitated by Prof. Manfred Ogris and Haider Sami, from the Division of Clinical Pharmacy and Diagnostics, University of Vienna, Vienna, Austria.

The authors declare no conflict of interest.

5 References

[1] Hedhammar, M., Alm, T., Gräslund, T., Hober, S., Single-step recovery and solid-phase refolding of inclusion body proteins using a polycationic purification tag. *Biotechnol. J.* 2006, *1*, 187–196.
[2] Wong, H. H., O'Neill, B. K., Middelberg, A. P., Centrifugal processing of cell debris and inclusion bodies from recombinant *Escherichia coli*. *Bioseparation* 1996, *6*, 361–372.
[3] Singh, S. M., Panda, A. K., Solubilization and refolding of bacterial inclusion body proteins. *J. Biosci. Bioeng.* 2005, *99*, 303–310.
[4] Chen, Y., Wang, Q., Zhang, C., Li, X. et al., Improving the refolding efficiency for proinsulin aspart inclusion body with optimized buffer compositions. *Protein Expression Purif.* 2016, *122*, 1–7.
[5] Burgess, R. R., Refolding solubilized inclusion body proteins. *Methods Enzymol.* 2009, *463*, 259–282.

[6] Dürauer, A., Mayer, S., Sprinzl, W., Jungbauer, A., Hahn, R., High-throughput system for determining dissolution kinetics of inclusion bodies. *Biotechnol. J.* 2009, *4*, 722–729.
[7] Grote, F., Ditz, R., Strube, J., Downstream of downstream processing – Integrated bioprocess development from upstream to downstream. *Chem. Ing. Tech.* 2009, *81*, 1276–1277.
[8] Freydell, E. J., Ottens, M., Eppink, M., van Dedem, G., van der Wielen, L., Efficient solubilization of inclusion bodies. *Biotechnol. J.* 2007, *2*, 678–684.
[9] Wellhoefer, M., Sprinzl, W., Hahn, R., Jungbauer, A., Continuous processing of recombinant proteins: Integration of inclusion body solubilization and refolding using simulated moving bed size exclusion chromatography with buffer recycling. *J. Chromatogr. A* 2013, *1319*, 107–117.
[10] Strandberg, L., Enfors, S. O., Factors influencing inclusion body formation in the production of a fused protein in *Escherichia coli*. *Appl. Environ. Microbiol.* 1991, *57*, 1669–1674.
[11] Datta, I., Gautam, S., Gupta, M. N., Microwave assisted solubilization of inclusion bodies. *Sustainable Chem. Proc.* 2013, *1*, 1–7.
[12] Datar, R. V., Cartwright, T., Rosen, C.-G., Process economics of animal cell and bacterial fermentations: A case study analysis of tissue plasminogen activator. *Biotechnology* 1993, *11*, 349–357.
[13] Castellanos-Mendoza, A., Castro-Acosta, R. M., Olvera, A., Zavala, G. et al., Influence of pH control in the formation of inclusion bodies during production of recombinant sphingomyelinase-D in *Escherichia coli*. *Microb. Cell Fact.* 2014, *13*, 1–14.
[14] Luo, J., Leeman, M., Ballagi, A., Elfwing, A. et al., Size characterization of green fluorescent protein inclusion bodies in *E. coli* using asymmetrical flow field-flow fractionation–multi-angle light scattering. *J. Chromatogr. A* 2006, *1120*, 158–164.
[15] Upadhyay, A. K., Murmu, A., Singh, A., Panda, A. K., Kinetics of inclusion body formation and its correlation with the characteristics of protein aggregates in *Escherichia coli*. *PLoS One* 2012, *7*, e33951.
[16] Margreiter, G., Messner, P., Caldwell, K. D., Bayer, K., Size characterization of inclusion bodies by sedimentation field-flow fractionation. *J. Biotechnol.* 2008, *138*, 67–73.
[17] Wong, H. H., O'Neill, B. K., Middelberg, A. P. J., Cumulative sedimentation analysis of *Escherichia coli* debris size. *Biotechnol. Bioeng.* 1997, *55*, 556–564.
[18] Agerkvist, I., Enfors, S.-O., Characterization of *E. coli* cell disintegrates from a bead mill and high pressure homogenizers. *Biotechnol. Bioeng.* 1990, *36*, 1083–1089.
[19] Taylor, G., Hoare, M., Gray, D. R., Marston, F. A. O., Size and density of protein inclusion bodies. *Nat. Biotechnol.* 1986, *4*, 553–557.
[20] Walther, C., Mayer, S., Sekot, G., Antos, D. et al., Mechanism and model for solubilization of inclusion bodies. *Chem. Eng. Sci.* 2013, *101*, 631–641.
[21] Elena, G.-F., Joaquín, S.-F., Esther, V., Antonio, V., Tunable geometry of bacterial inclusion bodies as substrate materials for tissue engineering. *Nanotechnology* 2010, *21*, 205101.
[22] Cano-Garrido, O., Rodríguez-Carmona, E., Díez-Gil, C., Vázquez, E. et al., Supramolecular organization of protein-releasing functional amyloids solved in bacterial inclusion bodies. *Acta Biomater.* 2013, *9*, 6134–6142.
[23] Moon, M. H., Lee, S., Sedimentation/steric field-flow fractionation: A powerful technique for obtaining particle size distribution. *J. Microcolumn Sep.* 1997, *9*, 565–570
[24] Peternel, Š., Jevševar, S., Bele, M., Gaberc-Porekar, V., Menart, V., New properties of inclusion bodies with implications for biotechnology. *Biotechnol. Appl. Biochem.* 2008, *49*, 239–246.
[25] Filipe, V., Hawe, A., Jiskoot, W., Critical evaluation of Nanoparticle Tracking Analysis (NTA) by NanoSight for the measurement of nanoparticles and protein aggregates. *Pharm. Res.* 2010, *27*, 796–810.
[26] Korz, D. J., Rinas, U., Hellmuth, K., Sanders, E. A., Deckwer, W. D., Simple fed-batch technique for high cell density cultivation of *Escherichia coli*. *J. Biotechnol.* 1995, *39*, 59–65.
[27] Lee, S. Y., High cell-density culture of *Escherichia coli*. *Trends Biotechnol.* 1996, *14*, 98–105.

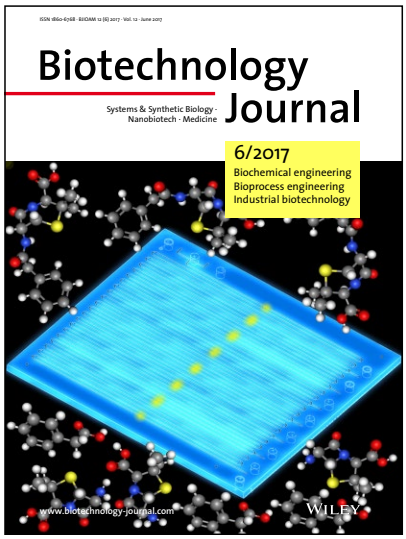

Cover illustration

Schematic representation of a microfluidic side-entry reactor with reactants of a penicillin G acylase reaction and pH sensors integrated along the reaction channel. The pH sensors enabled real-time monitoring of the reaction progress in a microfluidic reactor. Alkaline buffers added to the reactor's side-entries balanced the pH and increased product yield, thereby highlighting the feasibility of pH control. The cover is prepared by Pia Gruber, Marco P.C. Marques, Philipp Sulzer, Roland Wohlgemuth, Torsten Mayr, Frank Baganz and Nicolas Szita authors of the article "Real-time pH monitoring of industrially relevant enzymatic reactions in a microfluidic side-entry reactor (μSER) shows potential for pH control" (https://doi.org/10.1002/biot.201600475).

Biotechnology Journal – list of articles published in the June 2017 issue.